

## Supplementary Material

MoSe<sub>2</sub> embedded in (NiCo)Se<sub>2</sub> nanosheets to form heterostructure materials for high stability supercapacitors and efficient hydrogen evolution

Wenqiang Sun,<sup>a#</sup> Ziyang Liu,<sup>a#</sup> Dekun Liu,<sup>a</sup> Bona Zhang,<sup>b</sup> Yingjie Li,<sup>a</sup> Chenyong Wang,<sup>a</sup> Xingjia Liu,<sup>a</sup> Xiaofeng Wang,<sup>\*c</sup> Xue-Zhi Song,<sup>\*a</sup> and Zhenquan Tan <sup>\*a,b</sup>

<sup>#</sup>These authors contributed equally to this work.

<sup>a</sup> State Key Laboratory of Fine Chemicals, School of Chemical Engineering, Ocean and Life Sciences, Dalian University of Technology, Panjin 124221, China.

<sup>b</sup> Leicester International Institute, Dalian University of Technology, Panjin 124221, China.

<sup>c</sup> School of General Education, Dalian University of Technology, Panjin 124221, China.

\* Corresponding authors: Xiaofeng Wang: wangxf@dlut.edu.cn; Xue-Zhi Song: songxz@dlut.edu.cn; Zhenquan Tan: tanzq@dlut.edu.cn

## 1. Electrochemical analysis method

In order to obtain the performance of electrode materials as cathodes for supercapacitors, the electrode materials were measured by cyclic voltammetry (CV), constant current charge-discharge (GCD), and electrochemical impedance spectroscopy (EIS) ( $10^{-2}$  to  $10^5$ Hz) using the CHI660E electrochemical workstation (Chenhua Instrument Co., Shanghai, China). At room temperature, the electrochemical performance of the electrode was obtained using a standard three-electrode configuration in a 6 M KOH aqueous electrolyte. The prepared electrode material, foil wire electrode, and Hg/HgO were used as the working electrode, counter electrode, and reference electrode, respectively. In addition, the electrochemical performance of the assembled HSC device was tested in a two-electrode system using NCM-Se as the cathode material and AC as the anode material. To evaluate HER, the prepared electrode material was used as the working electrode, carbon rod was used as the counter electrode, and Hg/HgO electrode was used as the reference electrode. Linear sweep voltammetry (LSV) was performed at a scan rate of  $5 \text{ mV s}^{-1}$  in 1 M KOH electrolyte. To ensure consistency, all potentials were set to reversible hydrogen electrodes (RHE). To calculate the double layer capacitance ( $C_{dl}$ ) of electrode materials, the relationship curve between cyclic voltammetry (CV) and Hg/HgO was tested in the potential range of  $-0.4 \sim -0.3 \text{ V}$ , with a scanning rate range of  $20 \text{ mV s}^{-1}$  to  $100 \text{ mV s}^{-1}$ . Electrochemical impedance spectroscopy (EIS) is performed in the frequency range of  $10^{-2}$  to  $10^5$ Hz at  $-1.15 \text{ V}$ .

In the production of HSC device, (NiCo)Se<sub>2</sub>/MoSe<sub>2</sub>/NF and activated carbon (AC) were employed as the cathode and anode of HSC, respectively, with a cellulose paper serving as the separator. PVA/KOH was employed as the electrolyte. Among these materials, (NiCo)Se<sub>2</sub>/MoSe<sub>2</sub>/NF is utilized as the cathode, and the anode slurry is obtained by uniformly combining AC, carbon black (CB), and polytetrafluoroethylene (PTFE) in a mass ratio of 8:1:1 through ultrasonication. The quantity of AC is calculated using the formula (1):

$$q^+ = q^-, \frac{m_+}{m_-} = \frac{C_- \times \Delta U_-}{C_+ \times \Delta U_+} \quad (1)$$

where  $C$  is the specific capacitance and  $\Delta U$  is the potential window. And PVA/KOH electrolyte is prepared by combining 3 g of PVA, 30 mL of DIW and 6 mL of KOH (6 M) solution at 90 °C. The resulting mixture is then stirred in an oil bath until it reaches a gelatinous consistency.

The specific capacitance of different electrodes was calculated from the galvanostatic discharge curves using following equation (2) and (3):

$$C_a = \frac{2I \int U dt}{s \Delta U^2} \quad (2)$$

$$C_s = \frac{2I \int U dt}{m \Delta U^2} \quad (3)$$

where  $C_a$  ( $F \text{ cm}^{-2}$ ) is the areal capacitance,  $C_s$  ( $F \text{ g}^{-1}$ ) is specific gravimetric capacitance,  $I$  (A) is the discharge current,  $\int U dt$  is the enclosed area of the discharge curve,  $\Delta U$  is the voltage window,  $s$  ( $\text{cm}^2$ ) and  $m$  (g) are the effective area of the working electrode and the mass of the active material on the electrode, respectively.

The areal energy density  $E$  ( $\text{Wh Kg}^{-1}$ ) and power density  $P$  ( $\text{W Kg}^{-1}$ ) of the ASCs were calculated using eqs (4) and (5), respectively.

$$E = \frac{C_s \Delta U^2}{2 \times 3.6} \quad (4)$$

$$P = \frac{3600 \times E}{\Delta t} \quad (5)$$

All obtained potential values were calibrated to the reversible hydrogen electrode (RHE) according to the following equation (6):

$$E_{RHE} = E_{Hg/HgO} + 0.924 \quad (6)$$

The typical overpotential ( $\eta$ ) value was evaluated using the following equation (7):

$$\eta = -E_{RHE} \quad (7)$$

The Faraday efficiency (FE) is obtained by the formula (8) and (9):

$$FE = \frac{V_{experimental}}{V_{Theoretical}} \times 100\% \quad (8)$$

$$V_{Theoretical} = \frac{IRTt}{PzF} \quad (9)$$

where I: operating current density(mA cm<sup>-2</sup>);

R: universal gas constant(0.0821 atm. L mol<sup>-1</sup> K<sup>-1</sup>);

T: Fahrenheit (K) (value of 295.15 K);

P: atmospheric pressure (atm.) (value of 0.986 atm);

z: number of electrons involved in the production of 1 mole of H<sub>2</sub> (z=2);

F: Faraday's constant (F=96,485 C).

## 2. DFT calculation

First, a model of (NiCo)Se<sub>2</sub> with a space group P63/MMC is constructed, with lattice parameters, a= 6.3151 Å, b= 3.646 Å, c = 5.337 Å. α=β=γ=90°. The model cuts A surface with thickness of 2 along the direction (102) and introduces a 15 Å vacuum layer to obtain a 1 × 1 × 1 surface structure consisting of 6 Ni atoms, 2 Co atoms, 8 Se atoms. The surface structure of the lattice constant of a= 17.8987 Å, b= 3.4645 Å, c = 18.1648 Å. α=β=γ=90°.

The model of MoSe<sub>2</sub> with a space group P63/MMC is constructed. The lattice parameter alpha beta gamma a = 5.6967 Å, b = 3.289 Å, c = 12.927 Å, α=β=γ=90°. Cut the surface in direction (002), introduce 15 Å vacuum layer, a 1 × 1 × 1 surface structure consisting of 1 Mo atoms, 2 Se atoms is obtained. The lattice constants of the surface structure are a = 5.6967 Å, b = 3.289 Å, c = 12.927 Å, α=β=γ=90°.

The (NiCo)Se<sub>2</sub>@MoSe<sub>2</sub> heterostructure was constructed by combining 1 × 1 × 1 (NiCo)Se<sub>2</sub> monomer with 3 × 1 × 1 MoSe<sub>2</sub> monomer. The lattice constants of the two heterostructures are averaged, and a = 17.4988 Å, b = 3.3768 Å, c = 15.5459 Å. In order to determine the feasibility of heterostructure formation, the lattice mismatch rate δ is calculated as follows: δ = |a<sub>f</sub>-a<sub>s</sub>|/ a<sub>s</sub> \*100%, where a<sub>f</sub> is the lattice parameter a of MoSe<sub>2</sub>, and a<sub>s</sub> is the lattice parameter a of (NiCo)Se<sub>2</sub> as the substrate material, and the lattice mismatch rate is about 4.5%, less than 5%. This indicates that the interfacial strain during the formation of the heterogeneous structure is relatively small, indicating the feasibility of the formation of the heterogeneous structure.

The first-principles calculations are based on atomic spin polarization density

functional theory (DFT), which combines the Perdew-Burke-Ernzerhof (PBE) functional in the generalized gradient Approximation (GGA), using projection-enhanced wave (PAW) potential to characterize ionic nuclei. The truncation energy is based on the plane wave base set of 421.8 eV. The monkhorst 3x9x3 packet grid is used for sampling the Brillouin region, using a Gaussian smear method with a width of 0.1 eV to achieve partial occupation of the Kohn-Sham track. When the energy change drops below 10<sup>-5</sup>eV, the electron energy converges. When the force change is less than 0.02eV/Å, the geometric optimization is considered to have converged. The dispersion interaction was modeled by Grimme's DFT-D3 method. The adsorption energy ( $E_{\text{ads}}$ ) of OH<sup>-</sup> is defined as:

$$E_{\text{ads}} = E_{\text{OH}^-/\text{surf}} - E_{\text{surf}} - E_{\text{OH}^-}$$

Where  $E_{\text{OH}^-/\text{surf}}$  represents the OH<sup>-</sup> adsorption energy,  $E_{\text{surf}}$  represents the original surface energy, and  $E_{\text{OH}^-}$  represents the energy of isolated OH<sup>-</sup> in a vacuum system.

### 3. Supplementary data

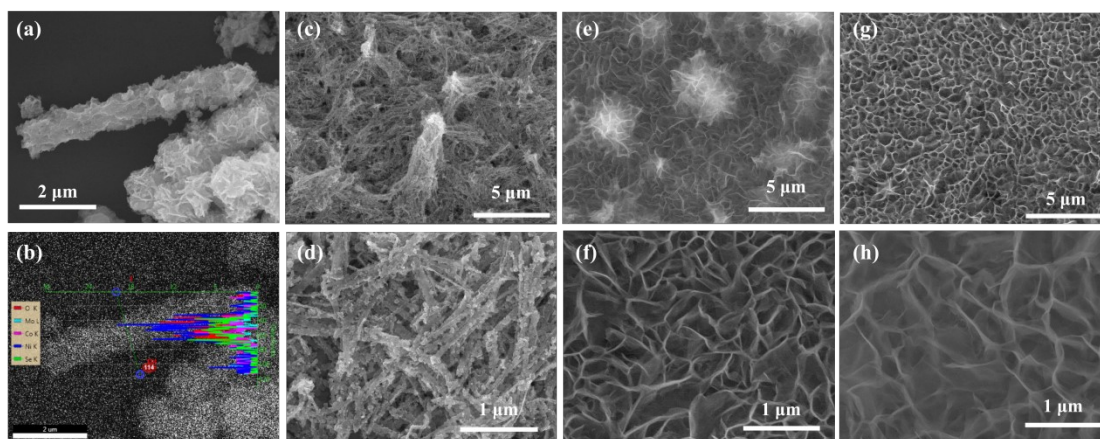


**Figure S1.** Scanning electron microscopy images of prepared (a-b)  $(\text{NiCo})\text{Se}_2/\text{MoSe}_2$  powder. (c-d)  $\text{NiSe}/\text{MoSe}_2$  powder. (e-f)  $\text{NiCo-LDH}/\text{NF}$ . (g-h)  $(\text{NiCo})\text{Se}_2/\text{NF}$ .

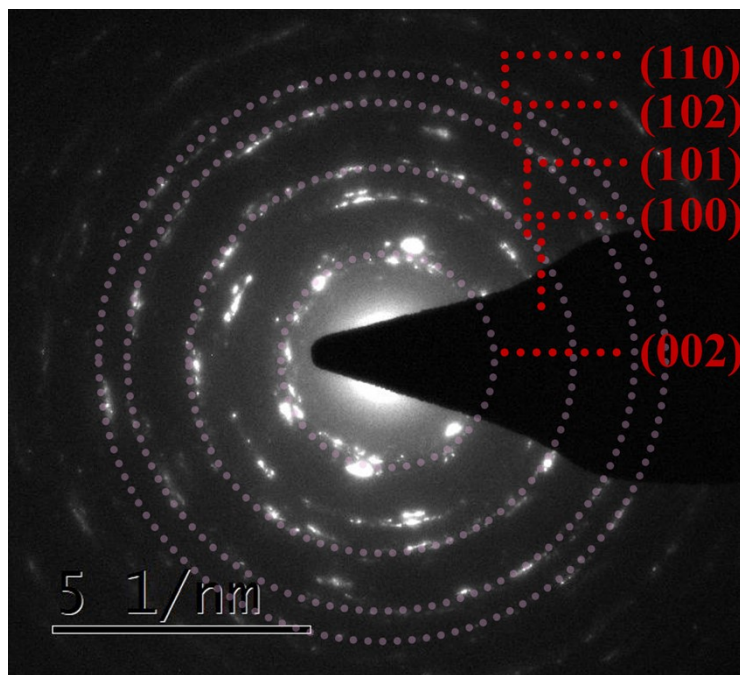


**Figure S2.** SAED pattern of  $(\text{NiCo})\text{Se}_2/\text{MoSe}_2$ . Among them, (002) and (100) are the characteristic crystal planes of  $\text{MoSe}_2$ , and (101), (102) and (110) are the characteristic crystal planes of  $(\text{NiCo})\text{Se}_2$ .

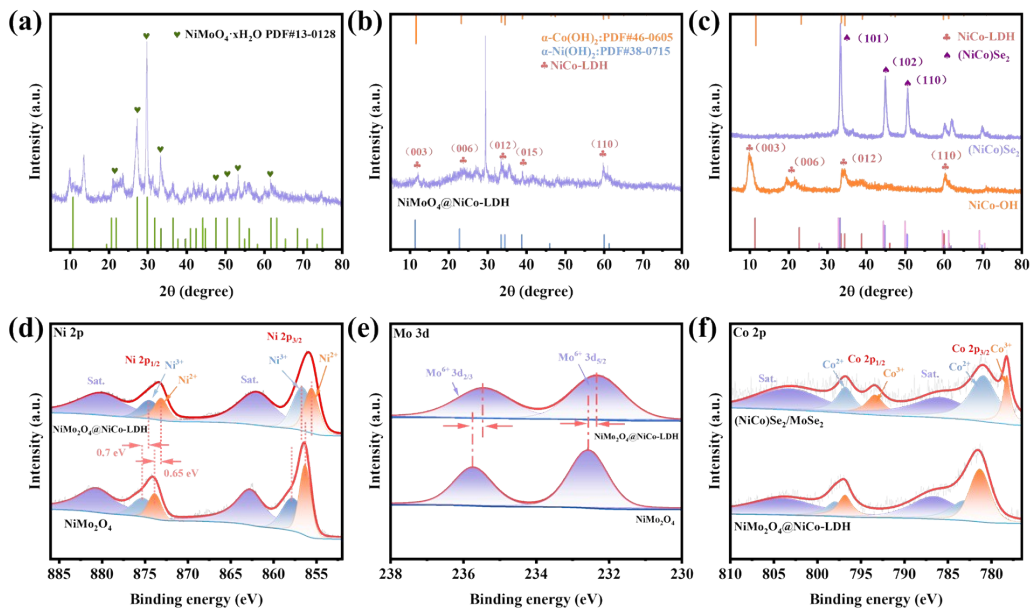


**Figure S3.** XRD patterns of (a)  $\text{NiMoO}_4/\text{NF}$ , (b)  $\text{NiMoO}_4@/\text{NiCo-LDH}/\text{NF}$  and (c)  $\text{NiCo-LDH}$  survey spectra of different electrode materials prepared in the article. The high-resolution XPS spectra of (d)  $\text{Ni } 2p$ , (e)  $\text{Co } 2p$ , (f)  $\text{Se } 3d$ .

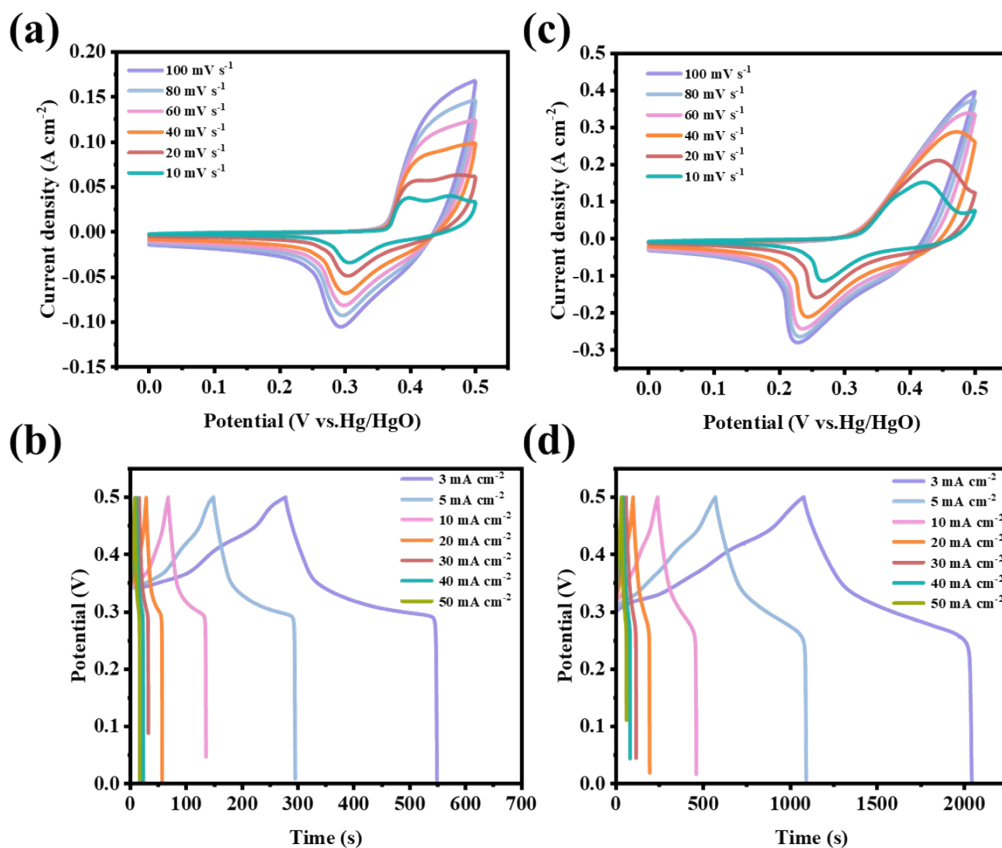


**Figure S4.** (a, c) CV and (b, d) GCD curves of  $\text{NiMoO}_4/\text{NF}$  and  $\text{NiMoO}_4@/\text{NiCo-LDH}/\text{NF}$ , respectively.

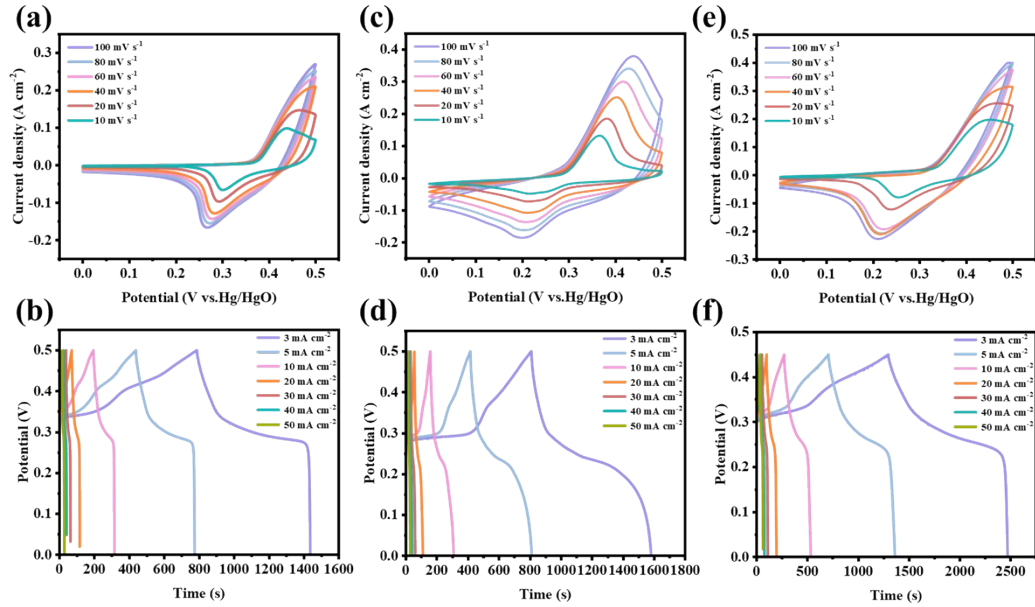


**Figure S5.** (a, c, e) CV and (b, d, f) GCD curves of NiSe/MoSe<sub>2</sub>/NF, NiCo-LDH/NF and (NiCo)Se<sub>2</sub>/NF respectively.

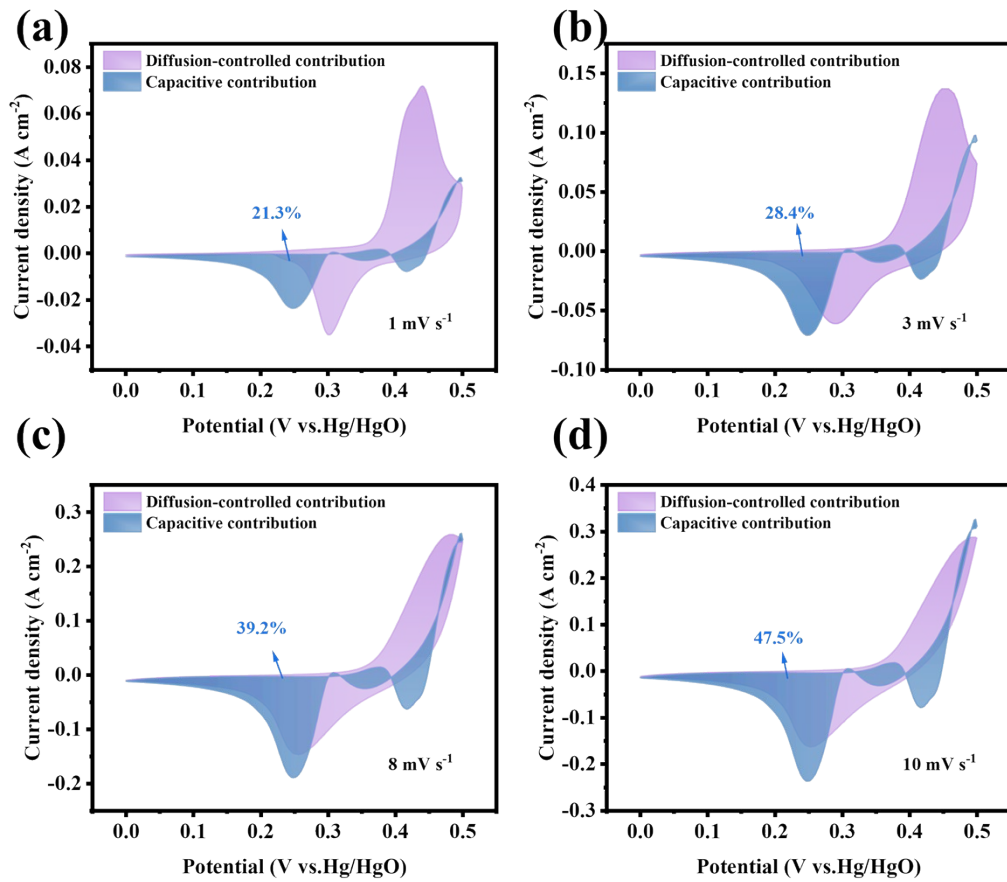


**Figure S6.** CV curves of (NiCo)Se<sub>2</sub>/MoSe<sub>2</sub>/NF at various scan rates.

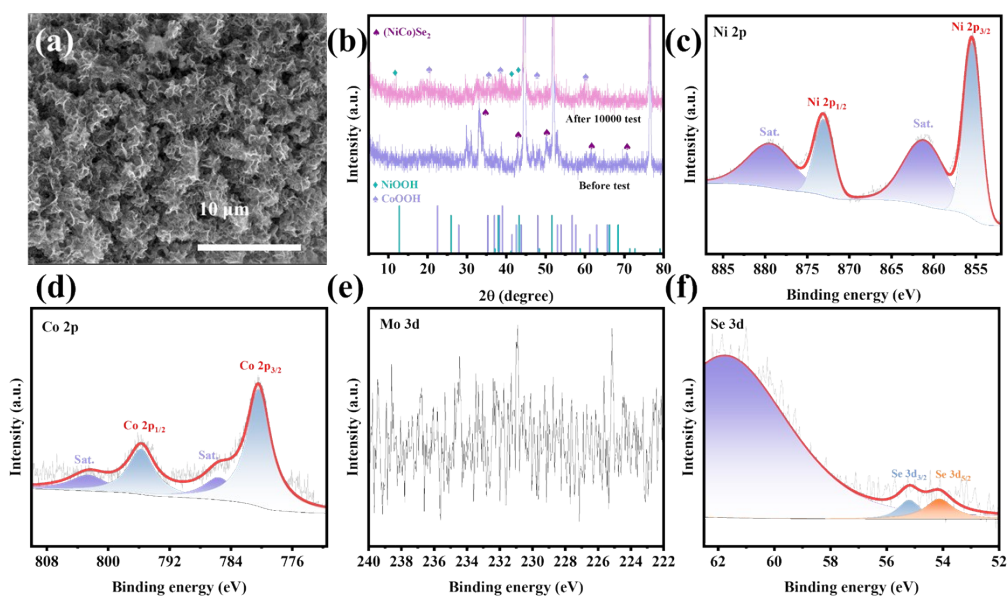


**Figure S7.** (a) SEM, (c)XRD, XPS spectra of (c) Co 2p (d) Ni 2p (e) Mo 3d (f) Se 3d of  $(\text{NiCo})\text{Se}_2/\text{MoSe}_2/\text{NF}$  after 10000 charge discharge cycles.

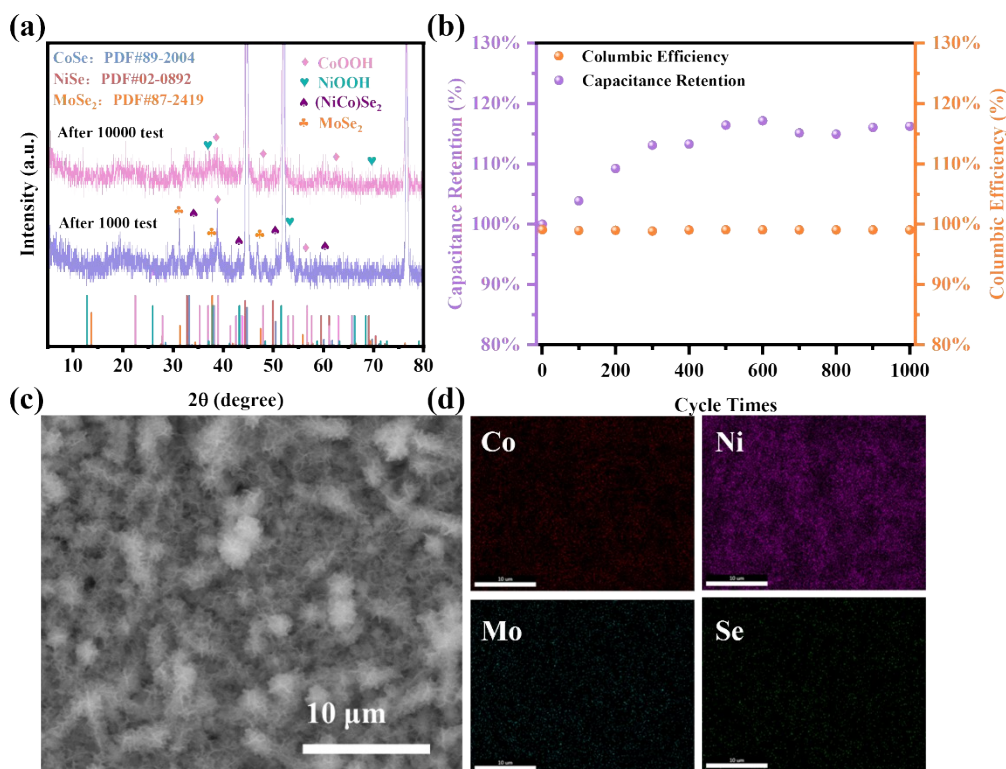


**Figure S8.** (a) XRD, (b) Capacitance Retention, (c) SEM, (d) ESD of  $(\text{NiCo})\text{Se}_2/\text{MoSe}_2/\text{NF}$  after 1000 charge discharge cycles.

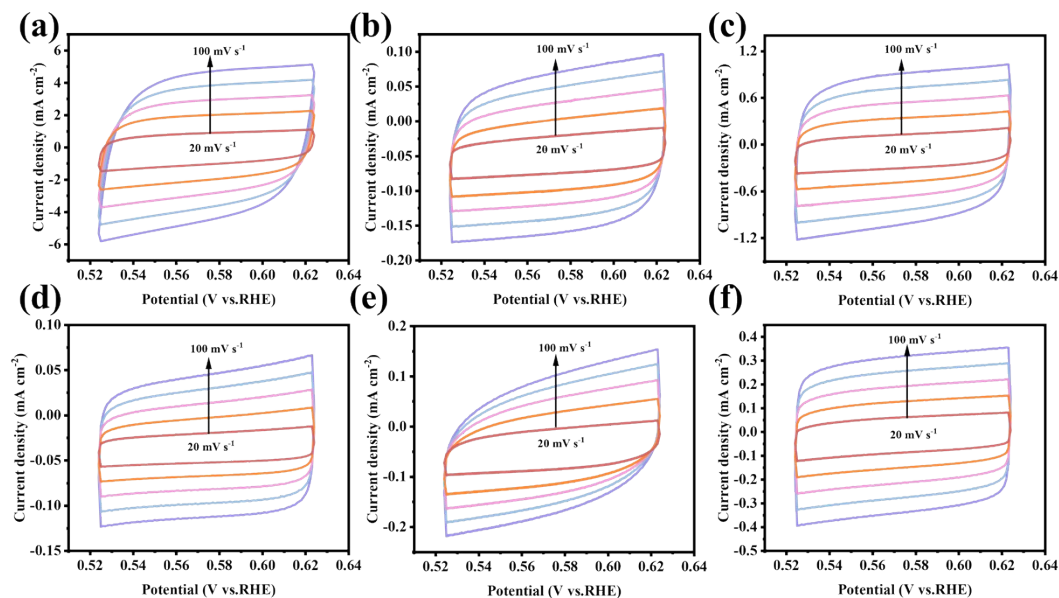


**Figure S9.** CV curves of (a)  $(\text{NiCo})\text{Se}_2/\text{MoSe}_2/\text{NF}$ ; (b)  $\text{NiCo-LDH}/\text{NF}$ ; (c)  $(\text{NiCo})\text{Se}_2/\text{NF}$ ; (d)  $\text{NiMoO}_4/\text{NF}$ , (e)  $\text{NiMoO}_4@/\text{NiCo-LDH}/\text{NF}$ , (f)  $\text{NiSe}/\text{MoSe}_2/\text{NF}$ .

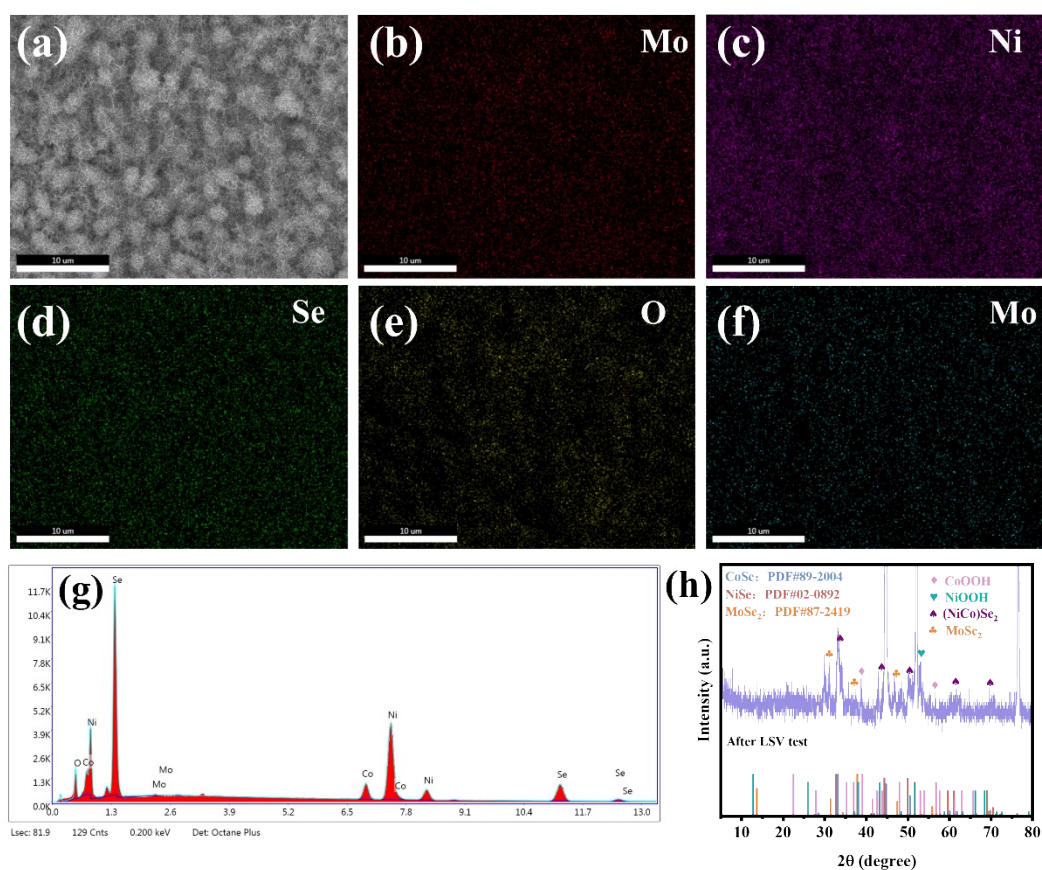


**Figure S10.** (a-g) SEM and EDS images; (h) XRD images of material  $(\text{NiCo})\text{Se}_2/\text{MoSe}_2/\text{NF}$  after HER stability testing

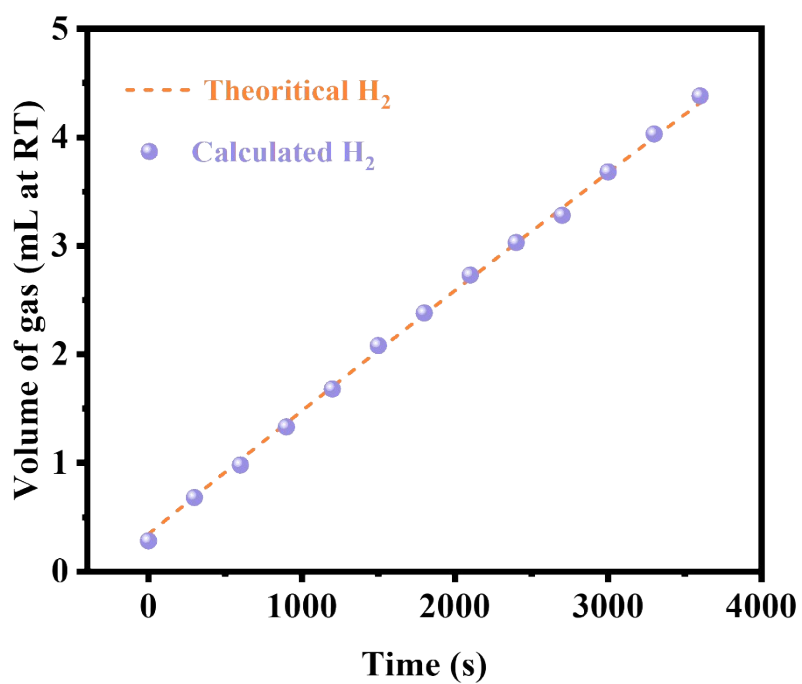


**Figure S11.** Faraday efficiency of material (NiCo)Se<sub>2</sub>/MoSe<sub>2</sub>/NF electrochemical HER